2005

Phosphoryl Transfer Step in the C-terminal Src Kinase Controls Src Recognition

Scot A. Lieser

Caitlin Shindler

Brandon E. Aubol

Sungsoo Lee
University of Rhode Island

Gongqin Sun
University of Rhode Island

See next page for additional authors

Citation/Publisher Attribution

Lieser, S. A., Shindler, C., Aubol, B. E., Lee, S., Sun, G., & Adams, J. A. (2005). Phosphoryl Transfer Step in the C-terminal Src Kinase Controls Src Recognition. *Journal of Biological Chemistry, 280*(9), 7769-7776. doi: 10.1074/jbc.M411736200
Available at: http://dx.doi.org/10.1074/jbc.M411736200

Phosphoryl Transfer Step in the C-terminal Src Kinase Controls Src Recognition

Authors

Scot A. Lieser, Caitlin Shindler, Brandon E. Aubol, Sungsoo Lee, Gongqin Sun, and Joseph A. Adams

THE JOURNAL OF BIOLOGICAL CHEMISTRY
Vol. 280, No. 9, Issue of March 4, pp. 7769–7776, 2005
Printed in U.S.A.

Phosphoryl Transfer Step in the C-terminal Src Kinase Controls Src Recognition*

Received for publication, October 15, 2004, and in revised form, December 9, 2004
Published, JBC Papers in Press, December 28, 2004, DOI 10.1074/jbc. M411736200

Scot A. Lieser‡, Caitlin Shindler§, Brandon E. Aubol‡¶, Sungsoo Lee‖, Gongqin Sun‖, and Joseph A. Adams§‡‡**

From the §Department of Pharmacology, University of California at San Diego, La Jolla, California 92093-0728, ‡Department of Chemistry & Biochemistry, University of California at San Diego, La Jolla, California 92093-0728, and ‖Department of Cell and Molecular Biology, University of Rhode Island, Kingston, Rhode Island 02881

All members of the Src family of nonreceptor protein tyrosine kinases are phosphorylated and subsequently down-regulated by the C-terminal Src kinase, Csk. Although the recognition of Src protein substrates is essential for a diverse set of signaling events linked to cellular growth and differentiation, the factors controlling this critical protein-protein interaction are not well known. To understand how Csk recognizes Src, the chemical/physical events that modulate apparent substrate affinity and turnover were investigated. Src is phosphorylated in a biphasic manner in rapid quench flow experiments, suggesting that the phosphoryl transfer step is fast and highly favorable and does not limit overall turnover. As opposed to other kinase-substrate pairs, turnover is not limited by the physical release of ADP based on stopped-flow fluorescence and catalytic trapping experiments, suggesting that other steps control net phosphorylation. The K_d for Src is considerably larger than the K_m based on single turnover kinetic and equilibrium sedimentation experiments. Taken together, the data are consistent with a mechanism whereby Csk achieves a low K_m for the substrate Src, not by stabilizing protein-protein interactions but rather by facilitating a fast phosphoryl transfer step. In this manner, the phosphoryl transfer step functions as a chemical clamp facilitating substrate recognition.

Src family nonreceptor protein tyrosine kinases regulate many essential processes involved in cellular growth and differentiation. All of the Src enzymes are distinguished by a characteristic arrangement of catalytic and noncatalytic domains. The tyrosine kinase domain of Src is flanked on the N-terminal end by two adaptor domains, the SH2[1] and SH3 domains. The regulation of the catalytic activity of Src has been widely studied, and it is now clear that a ubiquitously expressed nonreceptor protein tyrosine kinase, the C-terminal Src kinase (Csk), serves as the principal effector (1, 2). Csk phosphorylates a single residue in the C-terminal tail of Src (Tyr-527), an event that down-regulates catalytic activity. X-ray studies demonstrate that the phosphorylated tail of Src interacts with the SH2 domain, inducing a "closed" conformation of the enzyme (3–5). Curiously, although C-terminal phosphorylation causes dramatic effects on the activity of Src, it is still unclear how this intramolecular interaction influences the active site. Whereas Csk shares the same configuration of homologous SH2, SH3, and catalytic domains, it lacks a C-terminal tail sequence and is not regulated in the same manner as Src. X-ray data indicate that the SH2 domain in Csk docks to the small lobe of the kinase domain rather than to the large lobe as in Src (6). These differences in topology also lead to different roles for the SH2 domain. Although the SH2 domain in Src is associated with catalytic repression, this domain enhances catalysis by approximately two orders of magnitude in Csk (7).

Information transfer in the cell involves many different protein kinases, adaptor/scaffolding proteins, and subcellular structures that function cooperatively in large signaling complexes (8, 9). Therefore, investigations into protein-protein interactions are necessary for understanding how these sophisticated networks provide communication over defined spatial constraints. Whereas the biomolecular interaction between protein kinases and their target substrates is fundamentally important in understanding communication cascades, there is currently no three-dimensional structure of a kinase with a full-length protein substrate bound. Such a structure would be useful for determining how protein kinases use residue contacts both in and outside the active site to bind and phosphorylate proteins. Although high resolution x-ray structural data are not yet available, other studies have suggested that regions outside the active site play an important role in substrate recognition. For example, deletion analyses reveal that the interaction of Src with Csk relies only on residues within the Src kinase domain, suggesting that the SH2 and SH3 domains do not provide a binding surface for Csk (10). On the other hand, detailed mutagenesis studies have shown that several residues in helix αD of the Csk kinase domain offer critical binding determinants for Src recognition (11).

Csk efficiently phosphorylates the C terminus of Src, displaying a reported K_m of 1–5 μM (10–12). Comparatively, a 20-residue peptide based on the C-terminal tail of Src is very poorly phosphorylated with a K_m value that is ~100-fold larger than that for the full-length protein substrate (13). Such observations suggest that docking regions beyond the perimeter of the Csk active site, such as those in helix αD, assist in the recognition of physiological protein substrates (11). Whereas

* This work was supported by National Institutes of Health Grants GM 68168 (to J. A. A.) and 1P20 RR16457 and American Cancer Society Grant RSG-04-247-01-CDD (to G. S.). The costs of publication of this article were defrayed in part by the payment of page charges. This article must therefore be hereby marked "*advertisement*" in accordance with 18 U.S.C. Section 1734 solely to indicate this fact.
¶ Supported by National Institutes of Health Training Grant GM 07752.
** Supported by the Heme training grant.
‡‡ To whom correspondence should be addressed. Tel.: 858-822-3360; Fax: 858-822-3361; E-mail: joeadams@ucsd.edu.

[1] The abbreviations used are: SH2, Src homology-2; SH3, Src homology-3; Csk, C-terminal Src kinase; kdSrc, kinase-defective Src; MANT-ADP, ADP with *N*-methylanthraniloyl group attached to ribose ring; MANT-ATP, ATP with *N*-methylanthraniloyl group attached to ribose ring; MOPS, 3-(*N*-morpholino)propanesulfonic acid; AMPPNP, 5′-adenylyl-β,γ-imidodiphosphate.

some structural evidence has been uncovered in several cases (14, 15), what still remains unclear is how these docking regions promote low K_m values relative to peptide substrates. Previously, we showed that the yeast protein kinase Sky1p efficiently phosphorylates the RNA carrier protein, Npl3, in yeast using a chemical clamping mechanism (16). In this mechanism, the added recognition sites offered by the protein substrate are used to facilitate a rapid and highly favorable phosphoryl transfer step rather than selectively promote high affinity protein-protein interactions. This chemical step then serves to lower the K_m well below the K_d by prompting the conversion of substrate bound molecules to product. The avoidance of high affinity protein-protein interactions also optimizes substrate turnover by facilitating product release.

Could chemical clamping provide a general mechanism for substrate recognition within the protein kinase family? To examine this intriguing possibility, we studied the phosphorylation of Src by its principal regulator, Csk. Using fast-mixing techniques (rapid quench and stopped-flow fluorescence), we identified several key steps in the phosphorylation mechanism. Based on pre-steady-state and single turnover kinetic experiments, Csk phosphorylates Src using a pathway that is not limited by the direct transfer of the γ phosphate of ATP to the C terminus. The observation of fast ADP release in trapping experiments suggests that slow conformational changes may limit overall Src turnover. Through the identification of the phosphoryl transfer step, a lower limit on the real thermodynamic affinity (K_d) of Src and Csk could be established. The data indicate that the K_m for Src is considerably lower than the K_d because of the rapid phosphoryl transfer step. Csk does not utilize high affinity interactions that may be afforded through docking regions to stabilize the enzyme-substrate complex. Rather, the enzyme efficiently recognizes Src by utilizing these docking regions for the stabilization of the phosphoryl transfer step, a key hallmark of the chemical clamping mechanism.

EXPERIMENTAL PROCEDURES

Materials—ATP, ADP, MOPS, $MgCl_2$, KCl, acetic acid, DE52 resin, and liquid scintillant were obtained from Fisher Scientific. Mant-ATP and Mant-ADP were purchased from Molecular Probes. [γ-^{32}P]ATP was obtained from PerkinElmer Life Sciences.

Protein Purification—Full-length human Csk with a polyhistidine tag attached to the C terminus was expressed in *Escherichia coli* strain BL21(DE3) and purified with a Ni^{2+}-agarose column according to a previously published procedure (17). A mutant form of chicken Src lacking the first 82 residues and possessing a lysine-to-methionine substitution at position 295 (kdSrc) was coexpressed with GroEL/ES chaperonin proteins in *E. coli* strain BL21(DE3) and purified using a Ni^{2+}-agarose column according to a previously published procedure (11). Csk and kdSrc were determined to be pure by 12% SDS-PAGE. Csk concentrations were determined by the method of Gill and von Hippel (18). The concentration of kdSrc was determined by complete turnover experiments using catalytic amounts of Csk and excess [^{32}P]ATP. Both Csk and kdSrc were stored at −80 °C in 10 mM Tris, pH 8, 100 mM KCl, and 1 mM dithiothreitol.

Steady-state Kinetic Assays—Steady-state kinetic assays for Csk were determined using kdSrc as a substrate in the presence of 100 mM MOPS, pH 7.0, 100 mM KCl, 10 mM free Mg^{2+}, and 0.5 mM [γ-^{32}P]ATP (400–600 cpm pmol^{-1}). Assays were typically initiated by the addition of Csk to a mixture of kdSrc, $MgCl_2$, and ATP at 25 °C. The reaction mixtures (20 μl) were quenched with 30% acetic acid (180 μl). A portion of each reaction (180 μl) then was applied to DE 52 columns (3 ml of resin) and washed with 5 ml of 30% acetic acid. The collected flow-though containing phosphorylated substrate then was counted on the ^{32}P channel in liquid scintillant. Control experiments were performed to determine the background phosphorylation (*i.e.* phosphorylation of kdSrc in the presence of quench). The specific activity of [γ-^{32}P]ATP was determined by measuring the total counts of the reaction mixture. The time-dependent concentration of phosphorylated kdSrc then was determined by considering the total counts per minute of the flow-though, the specific activity of the reaction mixture, and the background phosphorylation. For steady-state kinetic measurements, product formation was linear with time and <5% substrate was converted to product.

Rapid Quench Flow Kinetic Assays—The phosphorylation of kdSrc was monitored using a KinTek Corporation quench flow apparatus model RGF-3 following a previously published procedure (16). Rapid quench flow experiments were typically executed by loading equal volumes of Csk and $MgCl_2$ into one sample loop and kdSrc, [γ-^{32}P]ATP (300–700 cpm pmol^{-1}), and $MgCl_2$ into the other loop in 100 mM MOPS, 100 mM KCl, pH 7. The reactions were quenched using 30% acetic acid, and phosphoproduct was separated from unreacted [^{32}P]ATP using the column separation assay. Control experiments were performed to determine the background phosphorylation (*i.e.* phosphorylation of substrate in the presence of quench) using previously published protocols (16). The time-dependent concentration of phosphoproduct then was determined by considering the total counts per minute of the flow-though, the specific activity of the reaction mixture, and the background phosphorylation.

Stopped-flow Fluorescence Experiments—All of the transient-state fluorescence studies were performed using an Applied Photophysics stopped-flow spectrometer. In the trapping experiments, Csk and ADP were preequilibrated in one 2.5-ml syringe and then mixed in a 1:1 ratio with Mant-ADP in the second 2.5-ml syringe. In the association experiments, Csk in one 2.5-ml syringe was mixed with Mant-ATP in the second 2.5-ml syringe. All of the experiments were performed at 25 °C in 100 mM MOPS, pH 7, 100 mM KCl in the presence of 10 mM free Mg^{2+} in both syringes. Fluorescence changes were monitored using an excitation wavelength of 290 nm and a 410-nm cut-on filter fitted between the cell and the photomultiplier tube. For data analysis, the average of 5–15 individual traces was recorded and the data were fit to double exponential functions.

Analytical Ultracentrifugation Experiments—The analytical ultracentrifugation experiments were performed with a Beckman Optima XL-I instrument using an An60Ti rotor. Both Csk and kdSrc, dialyzed in 100 mM MOPS, pH 7, 100 mM KCl, 1 mM dithiothreitol were run at a concentration of 5 μM. The mixture of Csk and kdSrc was run at equimolar concentrations of 5 μM. Absorbance changes as a function of radial position were measured at a rotor speed of 20,000 at 25 °C. Equilibrium was reached after 12 h at this rotor speed. The data were then analyzed using the Origin software package provided by Beckman. The program Sednterp (19) was used to calculate the partial specific volumes and solvent densities of both proteins based on their amino acid sequences.

Kinetic Data Analysis—The initial velocity *versus* substrate concentration data were fit to the Michaelis-Menten equation to obtain k_{cat} and K_m values for kdSrc. The production of phospho-kdSrc in the rapid quench flow experiments was fit to Equation 1,

$$[P] = \alpha \times [1 - \exp(-k_b t)] + L \times t \qquad \text{(Eq. 1)}$$

where [P] is the concentration of phospho-kdSrc, α is the amplitude of the "burst" phase, k_b is the burst phase rate constant, L is the linear rate constant, and t is time.

RESULTS

Steady-state Kinetic Parameters—For the kinetic studies in this paper, a mutant form of Src (K295M) was used as a substrate for Csk rather than the wild-type enzyme. This protein substrate (kdSrc) possesses no catalytic activity and thus cannot undergo autophosphorylation at the C-terminal tyrosine (Tyr-527) (11). The phosphorylation of kdSrc by Csk was monitored under steady-state reaction conditions by the addition of Csk (0.05 μM) to a mixture of [^{32}P]ATP (0.5 mM), 10 mM free Mg^{2+}, and varying amounts of kdSrc (1–10 μM). These mixtures then were allowed to react for 1–3 min and quenched with acetic acid, and the phosphorylated product was separated from unreacted [^{32}P]ATP using the DE52 column assay. Quantitative recovery of phospho-kdSrc from this column was verified by a separate autoradiographic PAGE assay (data not shown). Plots of initial velocity *versus* total Src concentration provide a k_{cat} of 0.2 ± 0.05 s^{-1} and a K_m of 5 ± 1 μM. Although the K_m value is similar to previous literature reports using kdSrc, the k_{cat} is ~4-fold lower (10, 11). The latter difference may be because of the differences in buffer components, pH, salt, and temperature between these assays and those published elsewhere (10, 11).

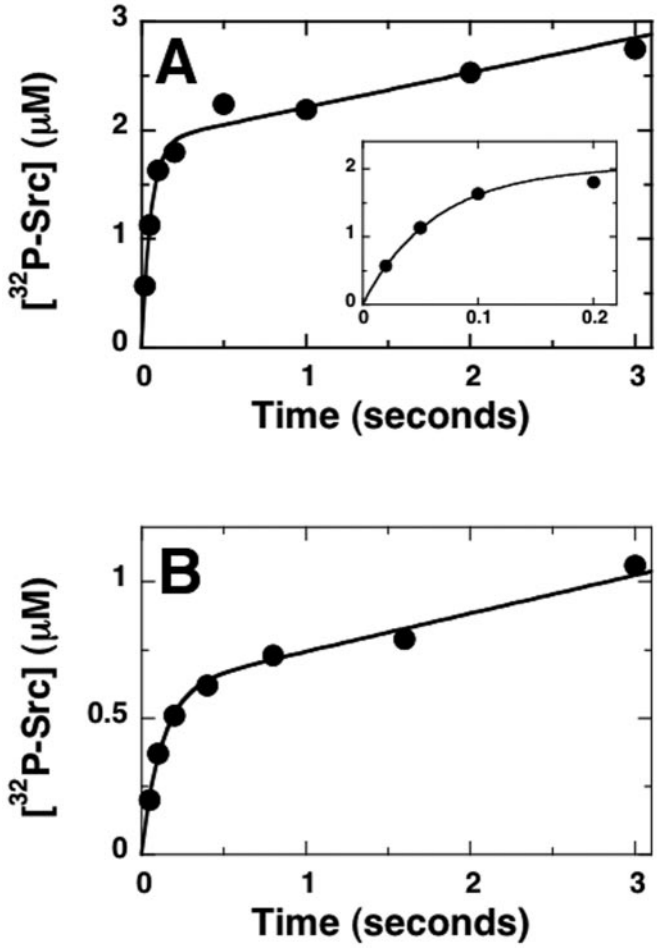

FIG. 1. **Pre-steady-state kinetic transients for Csk at two concentrations of kdSrc.** *A*, 10 μM kdSrc. Csk (8 μM) was mixed with an equal volume of [^{32}P]ATP (1 mM) and kdSrc (20 μM). The final concentrations of Csk and kdSrc in the reaction chamber are 4 and 10 μM. Fitting to Equation 1 provides values of 16 ± 2 s^{-1}, 2.0 ± 0.1 μM, and 0.32 ± 0.04 μM/s for k_b, α, and L, respectively. The *inset* shows the first 0.2 s of the reaction. *B*, 5 μM kdSrc. Csk (4 μM) was mixed with an equal volume of [^{32}P]ATP (1 mM) and kdSrc (10 μM). The final concentrations of Csk and kdSrc in the reaction chamber are 2 and 5 μM. Fitting to Equation 1 provides values of 9 ± 1 s^{-1}, 0.52 ± 0.04 μM, and 0.14 ± 0.02 μM/s for k_b, α, and L.

Pre-steady-state Kinetic Experiments—To determine whether the phosphoryl transfer step limits net turnover of kdSrc (k_{cat}), pre-steady-state kinetic experiments were performed using rapid quench flow methods. In this experiment, Csk (4 μM) was mixed with kdSrc (10 μM) and [^{32}P]ATP (0.5 mM) in the presence of 10 mM free Mg^{2+}. At discrete time intervals, the reaction was quenched with acetic acid and phospho-kdSrc was separated from unreacted [^{32}P]ATP using the DE52 column assay. As shown in Fig. 1*A*, the production of [^{32}P]kdSrc conforms to a biphasic kinetic pattern with a fast exponential (burst) phase followed by a slower linear phase. The data were fit to Equation 1 to obtain values of 16 ± 2 s^{-1}, 2.0 ± 0.1 μM, and 0.32 ± 0.04 μM/s for k_b, α, and L, respectively. The burst phase corresponds to the observed phosphoryl transfer rate constant, whereas the linear phase corresponds to the steady-state kinetic rate at 10 μM kdSrc. The data imply that the phosphoryl transfer step is much faster than net turnover ($k_b \gg k_{cat}$) and thus is not the rate-limiting step in the reaction.

The amplitude of the burst phase in Fig. 1*A* represents only 50% total Csk concentration (α = 2 μM, $[E]_{tot}$ = 4 μM). This substoichiometric amplitude is probably due to a low kdSrc concentration rather than to large amounts of inactive Csk.

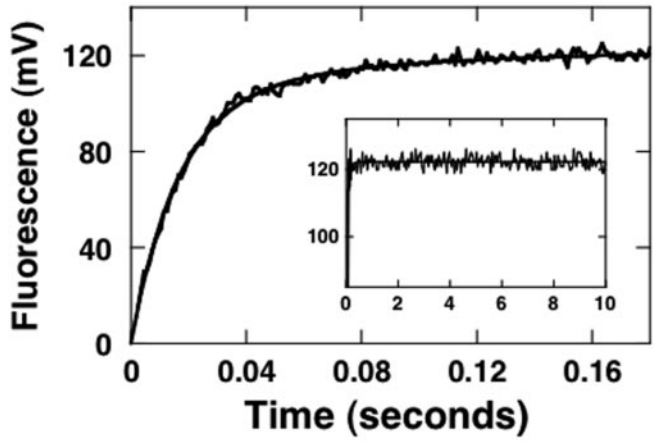

FIG. 2. **Dissociation rate constant for ADP from Csk.** Csk (1 μM) was preequilibrated with ADP (150 μM) in one syringe and then mixed with Mant-ADP (1 mM) from the second syringe of the stopped-flow fluorimeter. Both syringes contain 10 mM free Mg^{2+}. The final concentrations of Csk, ADP, and Mant-ADP are 0.5, 75, and 500 μM, respectively, in the mixing chamber. Fluorescence changes are monitored using a 410-nm cut-on filter (excitation 290 nm) and plotted as a function of time (0–0.18 s shown for clarity). The kinetic transient is fit to a double exponential function with rate constants of 61 ± 2 and 13 ± 4 s^{-1} and amplitudes of 100 ± 5 and 21 ± 4 mV, respectively. The *inset* shows the first 10 s of the reaction.

When the phosphoryl transfer step is fast ($k_b \gg k_{cat}$), the burst amplitude can be related to the total enzyme concentration ($[E]_{tot}$) by the following relationship: $\alpha = [E]_{tot}\{[S]/([S] + K_m)\}^2$ (20). This relationship predicts that α should correspond to 44% total enzyme concentration at 10 μM kdSrc, a value in keeping with the experimental findings of 50%. To provide further support for this conclusion, pre-steady-state kinetic experiments were performed at lower kdSrc (5 μM) and Csk (2 μM) concentrations. Under K_m concentrations of substrate, a burst amplitude of 26% was obtained (Fig. 1*B*), a value in line with the predicted amplitude of 25% based on the above relationship. With these substrate concentrations, the burst rate constant is lower (k_b = 9 ± 3 s^{-1}) than the constant at 10 μM kdSrc. Because of poor solubility, further pre-steady-state kinetic experiments above 10 μM substrate could not be performed to obtain the true phosphoryl transfer rate constant and the K_d for kdSrc and Csk.

Stopped-flow Trapping Experiments—To determine whether the release of ADP could participate in controlling the linear phase in Fig. 1, dissociation studies were performed using Mant-ADP as a trapping reagent (21–24). In the stopped-flow instrument, a preequilibrated mixture of Csk (1 μM) and ADP (150 μM) was mixed with Mant-ADP (500 μM in the mixing chamber) and fluorescence output above 410 nm was monitored. As shown in Fig. 2, the displacement of ADP by Mant-ADP is accompanied by a large fluorescence increase best fit to a double exponential function with rate constants of 61 ± 2 and 13 ± 4 s^{-1}. No further fluorescence changes are observed from 0.3 to 10 s (Fig. 2, *inset*). In control experiments, the omission of ADP led to no appreciable fluorescence change in the time frame of the trapping experiment (data not shown), indicating that the binding of Mant-ADP is fast on the stopped-flow time scale and does not limit the observed transient in Fig. 2. Be-

[2] An additional constraint on the K_m expression was made based on the pre-steady-state kinetic and single turnover data. For Csk, the ratio of the net product release and the association rate constants is much lower than K_m (*i.e.* $k_4/k_2 \ll K_m$) and can be omitted from the larger K_m expression. Because k_4 is 0.2 sec^{-1} based on k_{cat} and k_2 is a minimum of 0.9 μM^{-1} sec^{-1} based on S_{ST} (Fig. 5*B*), $k_4/k_2 \leq 0.2$ μM and is at least 25-fold lower than K_m (5 μM).

cause increasing the concentration of Mant-ADP from 500 to 800 μM did not alter the time-dependent fluorescence changes (data not shown), the observed transient reflects the true dissociation rate constant for ADP. To ensure that the initial concentration of Csk·ADP in the syringe does not influence the observed trapping kinetics, the ADP concentration was halved (75 μM) but no significant changes in the dissociation rate constant using 800 μM Mant-ADP were detected (data not shown). The detection of two kinetic phases in the trapping kinetics is consistent with the presence of more than one binary E·ADP complex as observed previously for other protein kinases (16, 21). However, both rates in the trapping experiments are much larger than Src turnover (0.2 s^{-1}), implying that the net release of ADP does not control turnover (k_{cat} = 0.2 s^{-1}).

Catalytic Trapping Experiments—To provide further evidence that ADP release is fast relative to k_{cat}, catalytic trapping experiments were performed. In these experiments, Csk was preequilibrated with ADP and then rapidly mixed with Src and excess ATP in the rapid quench flow instrument. If the release of ADP limits turnover ($k_{off} \approx k_{cat}$), the burst phase amplitude will disappear (25). In comparison, if the release of ADP is fast and does not limit turnover ($k_{off} \gg k_{cat}$), preequilibration with this product will not influence the burst phase. As shown in Fig. 3*A*, ADP preequilibration (300 μM) prior to reaction initiation does not influence the burst amplitude for kdSrc phosphorylation relative to the control lacking ADP. The data in the absence of ADP are fit to Equation 1 to obtain k_b, α, and L values of 10 ± 1 s^{-1}, 0.56 ± 0.10 μM, and 0.20 ± 0.03 μM/s, respectively. The observed kinetics are insensitive to the total trap concentration, because increasing ATP from 1 to 1.5 mM at a constant ratio of ATP/ADP had no effect relative to the control experiment with no ADP (Fig. 3*B*). Prior studies have shown that the K_i for ADP is 30 μM (26), so preequilibrated ADP concentrations of 300 and 450 μM ought to be sufficient to ensure that most of the enzyme is initially complexed with the product prior to mixing with excess ATP. Taken together with the stopped-flow trapping results (Fig. 2), ADP dissociates from the active site of Csk with a rate constant that greatly exceeds k_{cat}.

Mant-ATP Association Kinetics—Because the pre-steady-state kinetic transients in Fig. 1 are initiated with ATP, we wondered whether the binding of this nucleotide could limit the rate of the burst phase. To address this issue, the association kinetics of Mant-ATP were monitored. We have shown previously that Mant-ATP binds with similar affinity as ATP in the presence of Mn^{2+}, so this fluorescent analog probably represents a good surrogate for the natural nucleotide (27). As shown in Fig. 4*A*, a large time-dependent increase in fluorescence was observed upon mixing of Csk (0.5 μM) and Mant-ATP (5 μM) in the stopped-flow instrument. The data are best fit to a double exponential function with rate constants of 103 ± 7 and 25 ± 5 s^{-1}. To determine the association rate constant, the kinetic transients were measured as a function of Mant-ATP. As shown in Fig. 4*B*, the rate of the fast phase increased as a function of Mant-ATP, whereas no observable changes in the rate of the slower phase were detected over this concentration range. The slope of the fast phase in Fig. 4*B* corresponds to the apparent association rate constant for Mant-ATP, a value of 3.1 μM^{-1} sec^{-1}. If ATP possesses a similar association rate constant, we predict that the observed binding rate for ATP at 0.5 mM is over 1500 s^{-1} and therefore does not limit the burst phase rate in Fig. 1*A* (k_b = 16 s^{-1}). To provide further support for this conclusion, we performed pre-steady-state kinetic experiments under conditions where [^{32}P]ATP (0.5 mM) was pre-

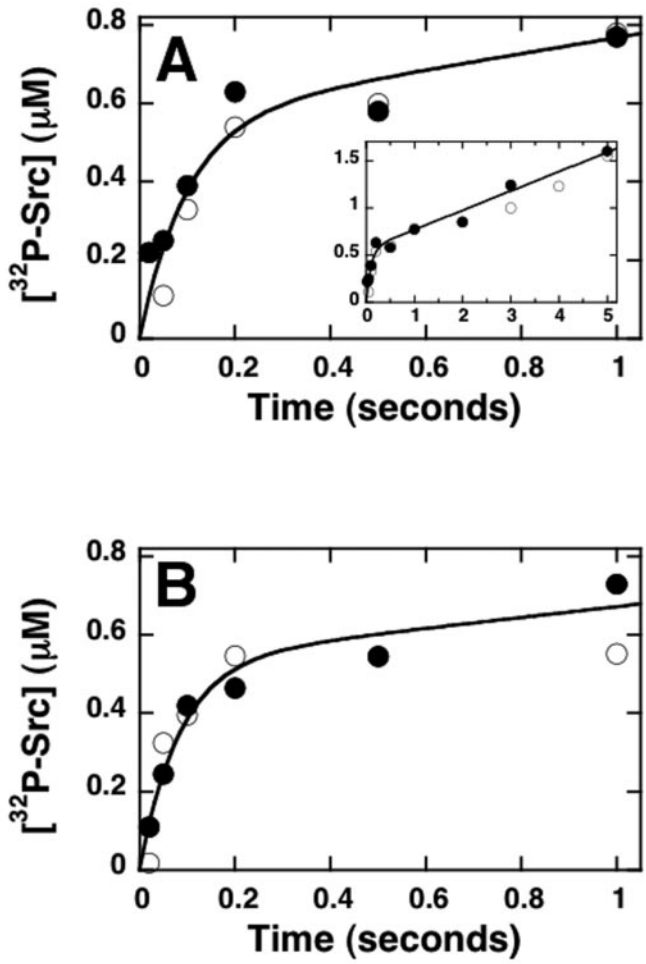

FIG. 3. **Catalytic trapping of ADP.** *A*, 300 μM ADP. In the rapid quench flow instrument, kdSrc (10 μM) and [^{32}P]ATP (2 mM) were mixed with an equal volume of Csk (4 μM) either in the absence (●) or presence (○) of 300 μM ADP. The final concentrations of Csk, kdSrc, [^{32}P]ATP, and ADP are 2 and 5 μM, 1 mM, and 150 μM, respectively. The data in the absence of ADP are fit to Equation 1 to obtain k_b, α, and L of 10 ± 1 s^{-1}, 0.56 ± 0.10 μM, and 0.20 ± 0.03 μM/s, respectively. The *inset* shows the linear phase of the reaction (0.5–5 s). *B*, 450 μM ADP. In the rapid quench flow instrument, kdSrc (10 μM) and [^{32}P]ATP (3 mM) were mixed with an equal volume of Csk (4 μM) either in the absence (●) or presence (○) of 450 μM ADP. The final concentrations of Csk, kdSrc, [^{32}P]ATP, and ADP are 2 and 5 μM, 1.5 mM, and 225 μM, respectively. The data in the absence of ADP are fit to Equation 1 to obtain k_b, α, and L of 12 ± 2 s^{-1}, 0.53 ± 0.03 μM, and 0.14 ± 0.03 μM/s, respectively.

incubated either with Csk (2 μM) or kdSrc (5 μM) before reaction initiation. No differences in burst rate were detected in either experiment (data not shown), suggesting that ATP binding does not limit the burst kinetics.

Single Turnover Kinetic Experiments—To assess the role of protein-protein interactions in controlling the magnitude of the burst phase in Fig. 1, the phosphorylation of kdSrc was measured under single turnover conditions where the total enzyme concentration exceeds that for the substrate. Under these constraints, the steady-state kinetic phase is avoided and the phosphoryl transfer step can be measured more directly (28). As shown in Fig. 5*A*, Csk (5 μM) was mixed with kdSrc (0.5 μM) in the rapid quench flow instrument and the amount of [^{32}P]kdSrc was monitored as a function of time. The substrate is phosphorylated in an exponential manner with an observed rate constant of 5 ± 0.5 s^{-1}. By comparison, the observed rate constant increases to 18 ± 1.7 s^{-1} at 20 μM Csk (Fig. 5*A*). Single turnover experiments can be used to obtain K_d values when the

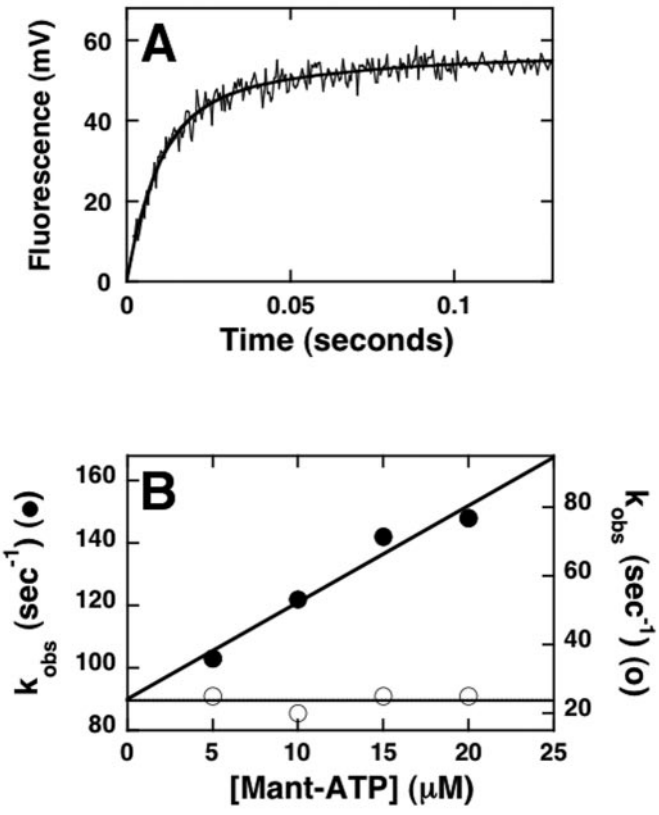

FIG. 4. **Association kinetics of Mant-ATP and Csk.** *A*, time-dependent fluorescence changes. Csk (1 μM) in one syringe was mixed with an equal volume of Mant-ATP (10 μM) from the second syringe in the stopped-flow instrument, and fluorescence changes were observed using a 410 nm cut-on filter (excitation 290 nm). The concentrations of Csk and Mant-ATP in the mixing chamber are 0.5 and 5 μM. The data are best fit to a double exponential function with rate constants of 103 ± 7 and 25 ± 5 s^{-1} and amplitudes of 39 ± 3 and 16 ± 2 mV, respectively. *B*, association rate constant measurement. Kinetic transients for the binding of Csk and Mant-ATP were measured at several Mant-ATP concentrations (5–20 μM). The fast phase rate constant (●) is plotted as a function of Mant-ATP and fit to a line function to obtain an observed association rate constant of 3.1 ± 0.5 μM^{-1} sec^{-1} and an intercept value of 90 ± 6 s^{-1}. The slow phase rate constant (○) did not vary over this concentration range.

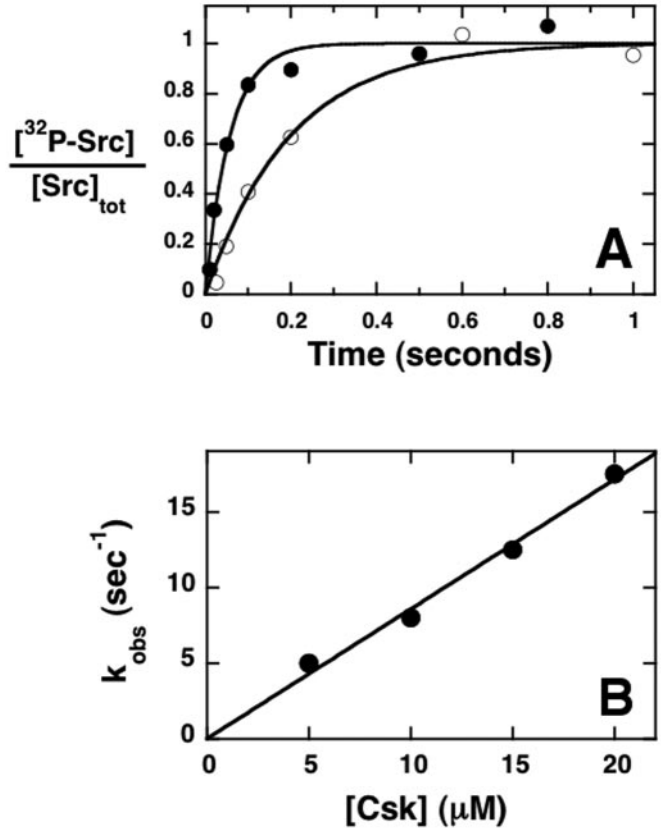

FIG. 5. **Single turnover kinetic analysis of kdSrc phosphorylation.** *A*, kinetic transients. In the reaction chamber of the rapid quench instrument, Csk at 5 (○) and 20 μM (●) was mixed with [^{32}P]ATP (0.5 mM) and kdSrc (0.5 μM at 5 μM Csk and 2 μM at 20 μM Csk). The quantity of [^{32}P]kdSrc normalized to the total kdSrc concentration is plotted as a function of time and fit to single exponential functions with rate constants of 5 ± 0.5 and 18 ± 1.7 s^{-1}. *B*, rate *versus* Csk. The single exponential rate constants at 5, 10, 15, and 20 μM Csk were determined from plots of [^{32}P]kdSrc *versus* time and then plotted as a function of total Csk concentration. The data best fit a line function with a slope (S_{ST}) of 0.9 ± 0.1 μM^{-1} sec^{-1}.

kinetic transients conform to single exponential functions over a range of enzyme concentrations (29), a condition satisfied in the present studies (Fig. 5*A*). Fig. 5*B* shows a plot of the observed single turnover rate constant as a function of total Csk concentration. The data show no signs of hyperbolic behavior in this concentration range, suggesting that the K_d for Csk and kdSrc greatly exceeds 20 μM, the highest concentration of Csk accessible in these experiments. Fitting the data to a linear function provides a slope value (S_{ST}) of 0.9 ± 0.1 μM^{-1} sec^{-1}. Under these conditions, S_{ST} corresponds to the apparent association constant for Csk and kdSrc, a value that exceeds k_{cat}/K_m (0.04 μM^{-1} sec^{-1}) by ~20-fold. Because S_{ST} is close in value to k_b/[Src] in Fig. 1, the interaction of Csk and kdSrc plays an important role in governing the rate of the burst phase.

Equilibrium Sedimentation Experiments—To determine whether Csk and kdSrc can form a stable complex at K_m values, we performed equilibrium sedimentation experiments on both free proteins and an equimolar mixture of Csk and kdSrc. As shown in Fig. 6, *A* and *B*, both Csk and kdSrc at 5 μM sedimented as monomeric species as expected. The data can be fit to obtain molar masses of 50,500 for Csk and 59,800 for kdSrc. These values are in line with the predicted molecular weights based on sequence data. As shown in Fig. 6*C*, a mixture of equal amounts of Csk and kdSrc (5 μM) results in a sedimentation curve that can be fit to a molar mass of 55,300, a value reflecting the average of both protein monomers. If both proteins form a stable complex, we anticipate an observed molecular weight of ~115,000. Such a complex would be expected to sediment according to the *dotted curve* in Fig. 6*C*. Sedimentation studies were also performed in the presence 50 μM AMPPNP (Fig. 6*D*). This sedimentation curve was fit to a molar mass of 54,300, indicating that this nucleotide did not assist in the formation of a stable complex at these concentrations. Similar results were also obtained with 50 μM ADP (data not shown). These sedimentation studies are conducted free of a solid support compared with previous pull-down assays (11) and therefore provide a very sensitive measure of complex formation in solution. Overall, the data suggest that, under K_m concentrations of both proteins, a stable complex does not appear to form at detectable levels.

DISCUSSION

The biomolecular interaction of Src family member nonreceptor protein tyrosine kinases with Csk is a regulatory event of fundamental importance in eukaryotic cells (30–32). The goals of the studies presented in this paper are to define the parameters of this protein-protein interaction and to determine what enzymatic factors control substrate recognition and turnover. Although there have been several detailed reports regard-

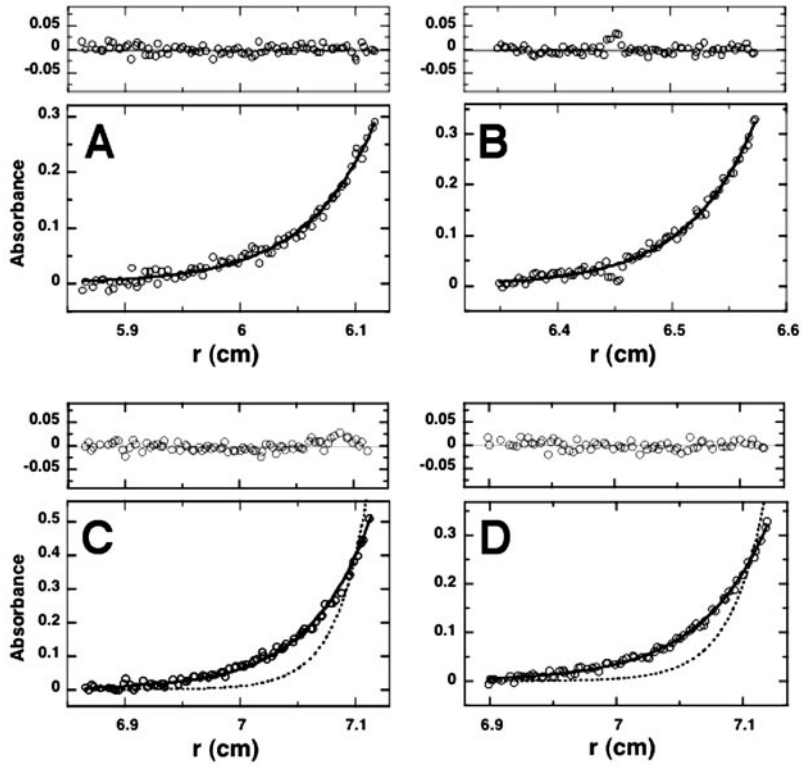

FIG. 6. **Equilibrium sedimentation of Csk and kdSrc.** Equal concentrations (5 μM) of Csk alone (*A*), kdSrc alone (*B*), Csk with kdSrc (*C*), and Csk with kdSrc and AMPPNP (50 μM) sedimented in the analytical ultracentrifuge for 14 h. The absorbance at 280 nm is plotted as a function of radial distance (cm). The data are fit to a monomer function in Origin, and the residuals are displayed above each plot. Molecular weights of 50,500 for Csk and 59,800 for kdSrc were obtained. The mixture of Csk and kdSrc with and without AMPPNP was fit to molecular weights of 55,300 in *panel C* and 54,300 in *panel D*. The *dotted lines* in these panels correspond to the predicted curve for the kdSrc·Csk complex with a molecular weight of 115,000.

ing the kinetics of Src phosphorylation by Csk (10, 11), they have not extended past preliminary steady-state kinetic measurements of K_m and k_{cat}. Whereas these parameters are important for defining catalytic efficiency, they do not provide direct information on the mechanism of protein phosphorylation and substrate recognition (33). For example, the K_m values for peptide substrates measured in steady-state kinetic assays oftentimes do not correlate with the intrinsic affinity (K_d) of the kinase-substrate pair (34, 35). These complexities diminish our ability to understand the molecular nature of substrate specificity within the protein kinase family. To overcome these problems, we employed fast-mixing kinetic procedures to Csk to isolate individual steps in the phosphorylation pathway of Src. From these individual steps, we can assemble a working model that defines how Csk interacts with Src proteins.

Csk Active Site Is Optimized for Efficient Phosphoryl Transfer—The application of fast-mixing methods to protein kinases one decade ago has allowed investigations into the role of the phosphoryl transfer step in controlling substrate processing in this important enzyme family (33). Original rapid quench flow experiments performed on cAMP-dependent protein kinase using a short peptide substrate (Kemptide, LRRASLG) revealed that the phosphoryl transfer step is ~20-fold faster than overall turnover (20), a parameter limited by ADP release (25). Since these findings, a looming question in the kinase field has centered on what factors control turnover using full-length physiological protein substrates. Recently, we showed that the phosphoryl transfer step in the yeast Sky1p is fast relative to turnover of its natural protein substrate Npl3 (16). Whether this mechanism is applicable to protein kinases and their protein substrates in mammalian systems is not yet clear. In a recent study, it has been shown that a truncated version of the transcription factor, MEF2A, is phosphorylated by ERK2 using a kinetic mechanism where the phosphoryl transfer step is partially rate-limiting (36), suggesting that the chemical step has some control on k_{cat}. In comparison to these findings, we found that the phosphoryl transfer step in Csk is considerably faster than k_{cat} (Fig. 1). Although it is not possible to saturate Csk with kdSrc to obtain an absolute value (Fig. 4), a lower limit of 20 s^{-1} can be placed on the phosphoryl transfer rate constant, a value that is ~100-fold larger than k_{cat}. Thus, the active site of Csk is optimally organized for rapid phosphorylation of the C terminus of Src. Later, we will address the role of this fast chemical step for the recognition of kdSrc.

Src Phosphorylation Is Not Limited by ADP Release—Although slow ADP release appears to limit substrate phosphorylation in many protein kinases (16, 20, 24, 34, 37–39), the trapping studies presented here are not consistent with such an event limiting Src phosphorylation (Figs. 2 and 3). These findings now raise an important question concerning the regulation of Src by Csk. If the phosphoryl transfer and ADP dissociation steps are fast, what controls turnover? Given the poor binding properties of Csk and kdSrc (Figs. 5 and 6), we cannot design a trapping experiment to measure directly a dissociation rate constant. However, if we assume that the proteins bind in a simple one-step reaction and that phosphorylation does not significantly affect protein affinity, an assumption that has some precedence (40), the dissociation rate constant for phospho-kdSrc can be estimated. Using a lower limit of 20 μM for the K_d and the apparent association rate constant for Csk and kdSrc (S_{ST} = 0.9 μM^{-1} sec^{-1}; see Fig. 5*B*), the dissociation rate constant for the two proteins should be in excess of 18 s^{-1}, a value much greater than k_{cat} (0.2 s^{-1}). However, achieving a stable enzyme-substrate or enzyme-product complex may require more than a simple bimolecular encounter. It is conceivable that one or more slow structural changes could be involved in protein binding, thereby limiting turnover. Given these considerations, we suggest that a conformational change unassociated with the phosphoryl transfer and ADP release steps is likely to play a significant role in limiting turnover.

Phosphoryl Transfer Step Controls Src Recognition—The present data indicate that Csk interacts very weakly with kdSrc yet somehow displays a low K_m for this protein substrate

SCHEME 1. **Src phosphorylation mechanism.**

($K_m \ll K_d$). By what mechanism does Csk convert a weak thermodynamic interaction into a low favorable K_m? To answer this question, it is important to understand the physical and chemical events in the active site of the enzyme. The phosphorylation of kdSrc can be depicted using the simple kinetic pathway in Scheme 1 where k_2 and k_{-2} are the association and dissociation rate constants for kdSrc, k_3 and k_{-3} are the forward and reverse rate constants for the phosphoryl transfer step, and k_4 is the net dissociation rate constant of both products (ADP and phospho-kdSrc) and any associated conformational changes. We have shown previously that the K_m equation for this pathway is rather complex but can be greatly simplified because of two primary experimental observations. First, the presence of a large burst rate constant and amplitude (Fig. 1) implies that the phosphoryl transfer step is fast and favorable ($k_4 < k_3 > k_{-3}$) (16, 20). Second, since the apparent association rate constant for kdSrc (S_{ST}) is much larger than k_{cat}/K_m (Fig. 4*B*), the rate of the reverse phosphoryl transfer step (i.*e.*ADP phosphorylation) must be fast relative to turnover ($k_{-3} > k_4$) (16). Under these conditions ($k_3 > k_{-3} > k_4$), the K_m for kdSrc can be related to K_d by the internal equilibrium constant for the phosphoryl transfer step ($K_{int} = k_3/k_{-3}$) as shown in Equation 2.[2]

$$K_m \approx \frac{K_d}{K_{int}} \qquad \text{(Eq. 2)}$$

A value of 20 for K_{int} has been determined for Csk using the Haldane relationship (41), a number similar to that found for other tyrosine kinases (42, 43). Using this K_{int} and Equation 2, the K_d for Csk and kdSrc is ~100 μM, a value consistent with our lower limit from single turnover data (Fig. 5*B*) and the inability to measure a stable enzyme-substrate complex in equilibrium sedimentation studies (Fig. 6). Overall, the data indicate that the K_m for kdSrc is ~20-fold lower than the K_d because of a fast and highly favorable phosphoryl transfer step.

CONCLUSIONS

Using fast-mixing methods, we demonstrated that the phosphorylation of kdSrc follows a unique mechanism where both the phosphoryl transfer and ADP release steps are fast and do not limit turnover. Instead, slow conformational changes are likely to control overall turnover. Whereas the kinetic studies cannot inform us on the nature of these changes, both crystallographic and solution studies show that Csk can adopt multiple conformations that could be linked with the dynamics of substrate turnover (6, 27, 44). Perhaps most interesting in this mechanism is the unusual binding affinity observed for the Csk·kdSrc complex. As depicted in Fig. 7, the interaction of Csk and kdSrc is surprisingly weak ($K_d \approx 100$ μM) with the complex exhibiting a high relative free energy under K_m concentrations of substrate. Despite the difficulties in forming a stable complex, Csk effectively recognizes kdSrc ($K_m = 5$ μM) by recruiting a highly efficient chemical step (chemical clamping step) that lowers K_m relative to K_d in accordance with the internal thermodynamics of the phosphoryl transfer reaction [ΔG_B]. Whereas the data collected over the last decade show that phosphoryl transfer in most protein kinases does not limit substrate turnover (33), the functional value of such a fast step has not been established. The data now show that this fast step can impact substrate recognition by facilitating phosphoprotein formation.

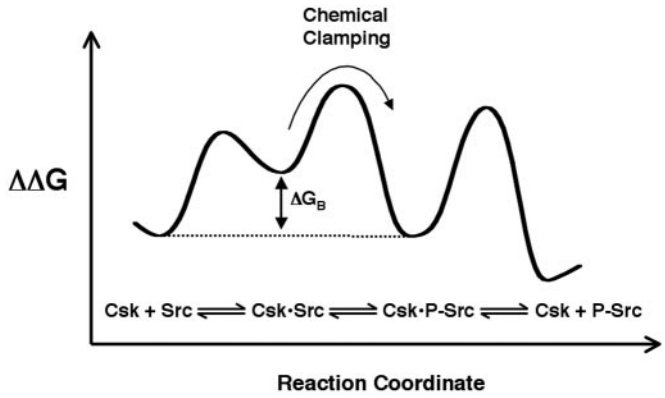

FIG. 7. **Chemical clamping mechanism for Src phosphorylation.** The reaction coordinate for kdSrc phosphorylation by Csk is displayed in relative energy terms under conditions where the concentration of kdSrc is fixed at the K_m (5 μM). In the reaction scheme at the bottom, ATP and ADP were omitted for clarity.

REFERENCES

1. Okada, M., Nada, S., Yamanashi, Y., Yamamoto, T., and Nakagawa, H. (1991) *J. Biol. Chem.* **266,** 24249–24252
2. Imamoto, A., and Soriano, P. (1993) *Cell* **73,** 1117–1124
3. Sicheri, F., Moarefi, I., and Kuriyan, J. (1997) *Nature* **385,** 602–609
4. Williams, J. C., Weijland, A., Gonfloni, S., Thompson, A., Courtneidge, S. A., Superti-Furga, G., and Wierenga, R. K. (1997) *J. Mol. Biol.* **274,** 757–775
5. Xu, W., Harrison, S. C., and Eck, M. J. (1997) *Nature* **385,** 595–602
6. Ogawa, A., Takayama, Y., Sakai, H., Chong, K. T., Takeuchi, S., Nakagawa, A., Nada, S., Okada, M., and Tsukihara, T. (2002) *J. Biol. Chem.* **277,** 14351–14354
7. Cole, P. A., Shen, K., Qiao, Y., and Wang, D. (2003) *Curr. Opin. Chem. Biol.* **7,** 580–585
8. Hunter, T. (1995) *Cell* **80,** 225–236
9. Pawson, T., and Scott, J. D. (1997) *Science* **278,** 2075–2080
10. Wang, D., Huang, X. Y., and Cole, P. A. (2001) *Biochemistry* **40,** 2004–2010
11. Lee, S., Lin, X., Nam, N. H., Parang, K., and Sun, G. (2003) *Proc. Natl. Acad. Sci. U. S. A.* **100,** 14707–14712
12. Takeuchi, S., Takayama, Y., Ogawa, A., Tamura, K., and Okada, M. (2000) *J. Biol. Chem.* **275,** 29183–29186
13. Ruzzene, M., Songyang, Z., Marin, O., Donella-Deana, A., Brunati, A. M., Guerra, B., Agostinis, P., Cantley, L. C., and Pinna, L. A. (1997) *Eur. J. Biochem.* **246,** 433–439
14. Brown, N. R., Noble, M. E., Endicott, J. A., and Johnson, L. N. (1999) *Nat. Cell Biol.* **1,** 438–443
15. Chang, C. I., Xu, B. E., Akella, R., Cobb, M. H., and Goldsmith, E. J. (2002) *Mol. Cell* **9,** 1241–1249
16. Aubol, B. E., Ungs, L., Lukasiewicz, R., Ghosh, G., and Adams, J. A. (2004) *J. Biol. Chem.* **279,** 30182–30188
17. Lin, X., Lee, S., and Sun, G. (2003) *J. Biol. Chem.* **278,** 24072–24077
18. Gill, S. C., and von Hippel, P. H. (1989) *Anal. Biochem.* **182,** 319–326
19. Laue, T. M., Shah, B. D., Ridgeway, T. M., and Pelletier, S. L. (1992) in *Analytical Ultracentrifugation in Biochemistry and Polymer Science* (Horton, J. C., ed) pp. 90–125, Royal Society of Chemistry, Cambridge, United Kingdom
20. Grant, B. D., and Adams, J. A. (1996) *Biochemistry* **35,** 2022–2029
21. Ni, Q., Shaffer, J., and Adams, J. A. (2000) *Protein Sci.* **9,** 1818–1827
22. Aubol, B. E., Nolen, B., Shaffer, J., Ghosh, G., and Adams, J. A. (2003) *Biochemistry* **42,** 12813–12820
23. Shaffer, J., Sun, G., and Adams, J. A. (2001) *Biochemistry* **40,** 11149–11155
24. Jan, A. Y., Johnson, E. F., Diamonti, A. J., Carraway, I. K., and Anderson, K. S. (2000) *Biochemistry* **39,** 9786–9803
25. Zhou, J., and Adams, J. A. (1997) *Biochemistry* **36,** 15733–15738
26. Grace, M. R., Walsh, C. T., and Cole, P. A. (1997) *Biochemistry* **36,** 1874–1881
27. Wong, L., Lieser, S., Chie-Leon, B., Miyashita, O., Aubol, B., Shaffer, J., Onuchic, J. N., Jennings, P. A., Woods, V. L., Jr., and Adams, J. A. (2004) *J. Mol. Biol.* **341,** 93–106
28. Johnson, K. A. (1998) *Curr. Opin. Biotechnol.* **9,** 87–89
29. Beebe, J. A., and Fierke, C. A. (1994) *Biochemistry* **33,** 10294–10304
30. Torgersen, K. M., Vang, T., Abrahamsen, H., Yaqub, S., and Tasken, K. (2002) *Cell. Signal.* **14,** 1–9
31. Mustelin, T., and Tasken, K. (2003) *Biochem. J.* **371,** 15–27
32. Latour, S., and Veillette, A. (2001) *Curr. Opin. Immunol.* **13,** 299–306
33. Adams, J. A. (2001) *Chem. Rev.***101,** 2271–2290
34. Adams, J. A., and Taylor, S. S. (1992) *Biochemistry* **31,** 8516–8522
35. Werner, D. S., Lee, T. R., and Lawrence, D. S. (1996) *J. Biol. Chem.* **271,** 180–185
36. Waas, W. F., Rainey, M. A., Szafranska, A. E., and Dalby, K. N. (2003) *Biochemistry* **42,** 12273–12286
37. Skamnaki, V. T., Owen, D. J., Noble, M. E., Lowe, E. D., Lowe, G., Oikonomakos, N. G., and Johnson, L. N. (1999) *Biochemistry* **38,** 14718–14730
38. Wang, C., Lee, T. R., Lawrence, D. S., and Adams, J. A. (1996) *Biochemistry* **35,** 1533–1539

39. Murray, B. W., Padrique, E. S., Pinko, C., and McTigue, M. A. (2001) *Biochemistry* **40,** 10243–10253
40. Qamar, R., Yoon, M. Y., and Cook, P. F. (1992) *Biochemistry* **31,** 9986–9992
41. Kim, K., and Cole, P. A. (1998) *J. Am. Chem. Soc.* **120,** 6851–6858
42. Boerner, R. J., Barker, S. C., and Knight, W. B. (1995) *Biochemistry* **34,** 16419–16423
43. McTigue, M. A., Wickersham, J. A., Pinko, C., Showalter, R. E., Parast, C. V., Tempczyk-Russell, A., Gehring, M. R., Mroczkowski, B., Kan, C. C., Villafranca, J. E., and Appelt, K. (1999) *Struct. Fold Des.* **7,** 319–330
44. Hamuro, Y., Wong, L., Shaffer, J., Kim, J. S., Stranz, D. D., Jennings, P. A., Woods, V. L., and Adams, J. A. (2002) *J. Mol. Biol.* **323,** 871–881

Phosphoryl Transfer Step in the C-terminal Src Kinase Controls Src Recognition

Scot A. Lieser, Caitlin Shindler, Brandon E. Aubol, Sungsoo Lee, Gongqin Sun and Joseph A. Adams

J. Biol. Chem. 2005, 280:7769-7776.
doi: 10.1074/jbc.M411736200 originally published online December 28, 2004
